A Computational Study on the Attack of Nitrogen and Oxygen Atoms to Toluene

Marzio Rosi[1(✉)], Stefano Falcinelli[1], Piergiorgio Casavecchia[2], Nadia Balucani[2], Pedro Recio[2], Adriana Caracciolo[2], Gianmarco Vanuzzo[2], Dimitrios Skouteris[3], and Carlo Cavallotti[4]

[1] Department of Civil and Environmental Engineering, University of Perugia, 06125 Perugia, Italy
{marzio.rosi,stefano.falcinelli}@unipg.it
[2] Department of Chemistry, Biology and Biotechnologies, University of di Perugia, 06123 Perugia, Italy
{piergiorgio.casavecchia,nadia.balucani, gianmarco.vanuzzo}@unipg.it
[3] Master-Tec, 06128 Perugia, Italy
[4] Department of Chemistry, Materials and Chemical Engineering, Politecnico di Milano, 20131 Milano, Italy
carlo.cavallotti@polimi.it

Abstract. The interaction between nitrogen atoms in their first electronically excited state ^{2}D and oxygen atoms in their ground state ^{3}P or in the first electronically excited state ^{1}D with toluene has been characterized by electronic structure calculations. We focused our attention, in particular, on the different sites of attack of nitrogen or oxygen to toluene using different methods. Our results suggest that, while for geometry optimizations DFT methods are adequate and different DFT methods provide comparable results, in order to compute accurate energies higher level of calculations, as CCSD(T), are necessary, in particular when strong correlation effects are present.

Keywords: Computational chemistry · Ab initio calculations · DFT methods · Combustion · Fuels · Chemistry of planetary atmospheres · Computational astrochemistry · Astrobiology

1 Introduction

Toluene represents the major aromatic found in gasoline. Development of detailed chemical kinetic models of toluene oxidation requires knowledge of the primary products and branching fractions (BFs) for the bimolecular reaction $O(^3P)+C_6H_5CH_3$ as a function of temperature (T) and pressure (p). Despite extensive kinetic studies [1–4], little is known about the mechanism and BFs for this reaction. We have therefore undertaken a synergistic experimental/theoretical investigation of $O(^3P)$+toluene by exploiting the same approach recently successfully used to identify all primary products and determine the

© Springer Nature Switzerland AG 2021
O. Gervasi et al. (Eds.): ICCSA 2021, LNCS 12953, pp. 620–631, 2021.
https://doi.org/10.1007/978-3-030-86976-2_42

BFs for the multichannel O(^{3}P) reactions with a variety of unsaturated aliphatic hydrocarbons [5–8], namely the crossed molecular beam (CMB) technique with soft electron ionization mass spectrometric detection and time-of-flight analysis. These experimental results are combined to high-level electronic structure calculations of the underlying triplet and singlet potential energy surfaces (PESs) and statistical RRKM/Master Equation computation of product distribution as a function of collision energy, E_c, as well as T and p, with intersystem crossing (ISC) taken into account, in order to get important information for improved kinetic modeling of toluene combustion.

Toluene is important also in other contexts, in particular in astrochemical contexts, as in the atmosphere of Titan which, being composed mainly by dinitrogen and simple hydrocarbons [9, 10], is somewhat reminiscent of the primordial atmosphere of Earth [11, 12]. Among the species identified by Cassini Ion Neutral Spectrometer (INMS) [13] in Titan atmosphere, benzene shows a relatively important mole fraction, being 1.3×10^{-6} at 950 km [14]. Toluene is efficiently produced in Titan's atmosphere since C_6H_5, the main product of the photodissociation of benzene, reacts with the radicals most abundant in Titan's atmosphere, which are H and CH_3 [15]. Molecular dinitrogen, in its closed shell electronic configuration, cannot react with hydrocarbons in the atmosphere of Titan because of the presence of relatively high activation energy barriers, but atomic nitrogen in its first electronically excited ^{2}D state can be produced [16] and it shows a significant reactivity with several molecules identified in the atmosphere of Titan. We have already investigated the reactions of N(^{2}D) with aliphatic hydrocarbons, like CH_4, C_2H_2, C_2H_4, C_2H_6 [17–22]. More recently, we started the investigation of the reaction between N(^{2}D) and aromatic hydrocarbons like benzene [23–25]. In this study we will report preliminary calculations on the interaction of N(^{2}D) with toluene comparing the attack of N(^{2}D) with that of O(^{3}P) or O(^{1}D) to toluene, paying attention to the computational requirements. Indeed, the ab initio study of these systems is computationally very challenging and a compromise between chemical accuracy and computational resources is necessary.

2 Computational Details

The stationary points, both minima and transition states, were localized on the Potential Energy Surface (PES) performing Density Functional Theory (DFT) calculations using the ωB97X-D [26, 27] or the B3LYP [28, 29] functional, in conjunction with the 6-311+G(d,p) basis set [30, 31]. The Basis Set Superposition Error (BSSE) has been previously estimated and computed to be 1.1 kcal/mol [24]. At the same level of theory we have computed the harmonic vibrational frequencies. The assignment of the saddle points was performed using intrinsic reaction coordinate (IRC) calculations [32, 33]. The geometry of all the species was optimized without any symmetry constraints. For all the stationary points, the energy was computed also at the higher level of calculation CCSD(T) [34–36] using the correlation consistent aug-cc-pVTZ basis set [37] and the DFT optimized geometries, following a previously applied computational scheme [38–49]. Both the DFT and the CCSD(T) energies were corrected to 0 K by adding the zero point energy correction computed using the scaled harmonic vibrational frequencies evaluated at DFT level. The energy of N(^{2}D) was estimated by adding the experimental [50] separation N(^{4}S) − N(^{2}D) of 55 kcal mol^{-1} to the energy of N(^{4}S) at all levels of

calculation. All calculations were done using Gaussian 09 [51] while the analysis of the vibrational frequencies was performed using Molekel [52, 53].

3 Results and Discussion

3.1 N(^{2}D) + Toluene

Figure 1 reports the optimized geometries of the isomers deriving from the interaction of N(^{2}D) with toluene. We have three different isomers depending on the carbon atoms interacting with nitrogen. Nitrogen forms two σ bonds with two adjacent carbon atoms, as expected because nitrogen has two electrons with opposite spin in different p orbitals which can interact with the two electrons with opposite spin involved in the π bond of the two carbon atoms. The energy required for breaking the π bond is more than compensated by the energy associated to the formation of the two σ bonds between nitrogen and carbon. The breaking of the π bond is shown by the C—C bond distance reported in Fig. 1 which corresponds to that of a single bond for the carbon atoms interacting with nitrogen. In Fig. 1 we have reported both the optimized geometry at B3LYP/6-311+G(d,p) and at ωB97XD/6-311+G(d,p) level in order to compare the two functionals. From Fig. 1 we can notice that the optimized geometries obtained with the two functionals are very similar, the difference in bond distances being within 0.01 Å and that in bond angles within 1°. In Table 1 we have reported the relative energies of these species with respect to N(^{2}D) + toluene computed both at DFT level and at the more accurate CCSD(T) level. From Table 1 we can notice that the three isomers are almost degenerate, with a slight preference for 2NMIN1. We can also notice that the binding energy of N(^{2}D) to toluene at DFT level is slightly higher at ωB97XD/6-311+G(d,p) level with respect to the B3LYP/6-311+G(d,p) level, the difference being however less than 2 kcal/mol. At the more accurate CCSD(T) level the binding energies computed using the two different optimized geometries are almost the same, the difference being less than 0.5 kcal/mol. At the B3LYP/6-311+G(d,p) level when N(^{2}D) interacts with toluene there is the formation of an initial van der Waals adduct, whose geometry is shown in Fig. 2. We can notice that the distance between the nitrogen and the closest carbon is 3.03 Å, while the binding energy is computed to be 30.2 kcal/mol at the B3LYP/6-311+G(d,p) level, as reported in Table 1. This value is very high for a van der Waals interaction, confirming that the B3LYP functional tends to overestimate the long range interactions. This adduct (2NMIN0) isomerizes to 2NMIN1 through the saddle point whose geometry is reported in Fig. 2; the barrier height for this isomerization is 2.6 kcal/mol, as reported in Table 1. It was not possible to localize on the PES this adduct at ωB97XD/6-311+G(d,p) level. This is similar to what recently found by Chin et al. for N(^{2}D) + benzene [54]: they were not able to find any initial adduct at ωB97XD/6-311+G(d,p) level, while our group could localize this adduct at B3LYP/6-311+G(d,p) level [24]. It is well known that B3LYP cannot describe very accurately dispersion forces and it is possible that it somewhat overestimates weak interactions.

Starting from 2NMIN1 we can consider the H loss and CH_3 loss channels; in Fig. 3 we have reported the optimized geometries for the transition states and the products, computed both at ωB97XD/6-311+G(d,p) and at B3LYP/6-311+G(d,p) levels, while in Table 1 we have reported the enthalpy changes and barrier heights for these reactions.

From Fig. 3 we can notice that the optimized geometries obtained with the two methods are comparable, the only significant difference being in the breaking bond. Since this bond (C—C in the CH_3 loss and C—H in the H loss) is almost broken the dependence of the energy from the distance is very small and the localization of the minimum is more difficult. From Table 1 we can notice that the DFT methods tends to overestimate the binding energies with respect to the values computed at CCSD(T) level, with the B3LYP results in slight better agreement with the more accurate CCSD(T) results.

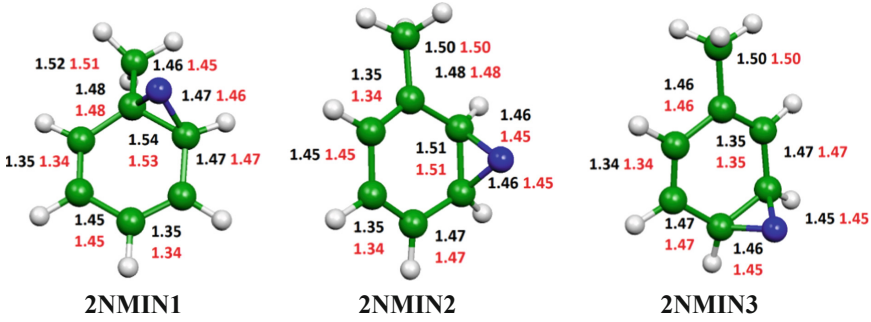

Fig. 1. Optimized geometries at B3LYP/6-311+G(d,p) (in black) and ωB97XD/6-311+G(d,p) (in red) level of the minima for the attack of N(^{2}D) to toluene. Bond lengths in Å. Carbon in green, nitrogen in blue, hydrogen in white. (Color figure online)

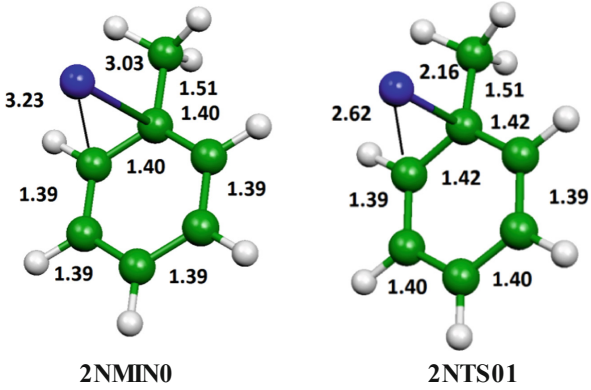

Fig. 2. Initial attack of N(^{2}D) to toluene in *ipso*. Optimized geometries at B3LYP/6-311+G(d,p). Bond lengths in Å. Carbon in green, nitrogen in blue, hydrogen in white. (Color figure online)

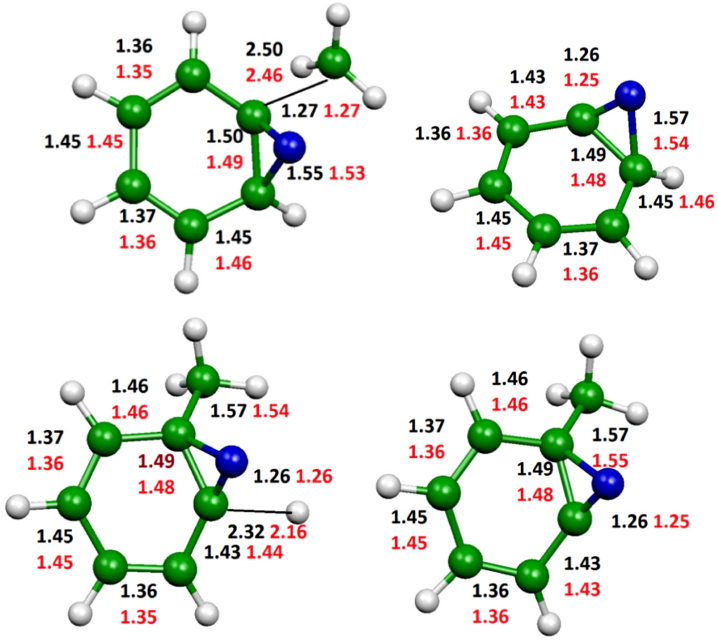

Fig. 3. Optimized geometries at B3LYP/6-311+G(d,p) (in black) and ωB97XD/6-311+G(d,p) (in red) level of the stationary points for the exit channels leading to CH_3 or H from 2NMIN1. Bond lengths in Å. Carbon in green, nitrogen in blue, hydrogen in white. (Color figure online)

3.2 $O(^3P)$ + Toluene

In Fig. 4 we have reported the optimized geometries of the isomers obtained from the interaction of $O(^3P)$ and toluene. The $O(^3P)$ interacts only with one carbon atom, since it has the two electrons in singly occupied p orbitals with parallel spin; these electrons cannot break a π bond and form two σ bonds with two adjacent carbon atoms, like $N(^2D)$. There are therefore four possible isomers, depending on the site of attack of the oxygen: *ipso*, *ortho*, *meta* and *para* with respect to the carbon center bonded to CH_3. For all isomers, there is first the formation of a van der Waals adduct which isomerizes, through a transition state, to the stable minimum. Figure 4 shows the optimized geometries computed at ωB97XD/6-311+G(d,p) level for all these species; for the *ipso* isomer we have optimized the geometries also at B3LYP/6-311+G(d,p) level, for comparison. In Table 2 we have reported the enthalpy changes and barrier heights for these reactions. From Fig. 4 considering the *ipso* isomer, we can notice that the optimized geometries at ωB97XD/6-311+G(d,p) level and at B3LYP/6-311+G(d,p) level compare very well, the only significant difference being in the distance between oxygen and carbon in the van der Waals adduct. From Table 2 we can notice that the binding energies of the four isomers are very similar, although the *ipso* isomer is slightly more stable than the others. It is also interesting to notice that the formation of all four isomers shows at CCSD(T) level an energy barrier above the reactants. From Table 2 we can notice also that the *ipso* isomer can loose a methyl radical in an exothermic reaction, while the loss

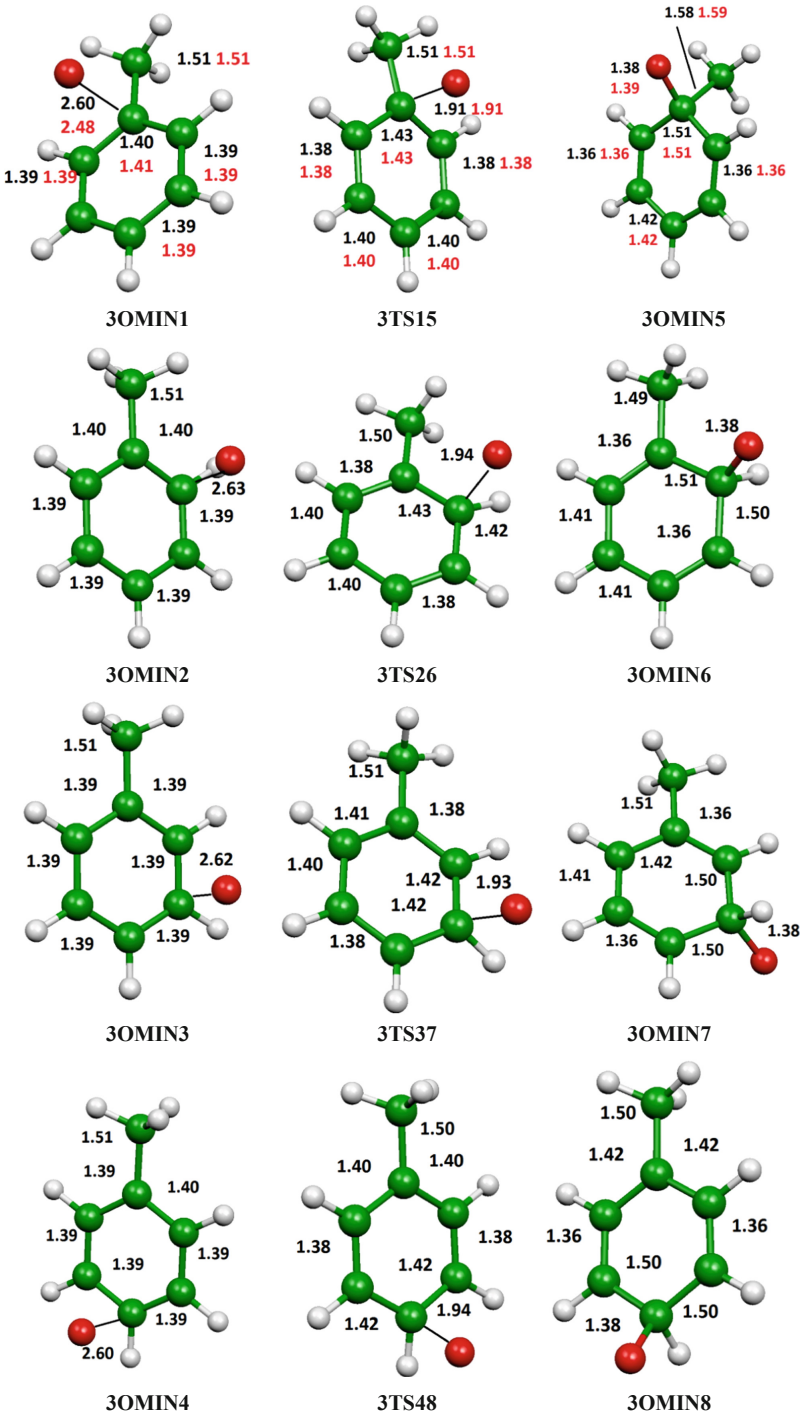

Fig. 4. Optimized geometries at ωB97XD/6-311+G(d,p) (in black) and B3LYP/6-311+G(d,p) (in red) level of the initial van der Waals adducts, the saddle points and the minima for the attack of O(^{3}P) to toluene. Bond lengths in Å. Carbon in green, oxygen in red, hydrogen in white. (Color figure online)

of an hydrogen atom from the *ortho*, *meta* or *para* isomers is an almost thermoneutral process, but with an energy barrier higher than 10 kcal/mol. In Fig. 5 we have reported the optimized geometries of the saddle points for the loss of CH_3 from the *ipso* isomer and for the loss of H from the *ortho* isomer. In both cases CH_3 or H leave the system in a direction almost perpendicular with respect to the plane of the molecule.

3.3 $O(^1D)$ + Toluene

Figure 6 reports the optimized geometries of the isomers deriving from the interaction of $O(^1D)$ with toluene. We have three different isomers depending on the carbon atoms interacting with oxygen. $O(^1D)$ forms two σ bonds with two adjacent carbon atoms, as expected because it has two electrons with opposite spin in different p orbitals which can interact with the two electrons with opposite spin involved in the π bond of the two carbon atoms. The energy required for breaking the π bond is more than compensated by the energy associated to the formation of the two σ bonds between oxygen and carbon. The breaking of the π bond is shown by the C—C bond distance reported in Fig. 6 which corresponds to that of a single bond for the carbon atoms interacting with oxygen. In Table 2 we have reported the relative energies of these isomers with respect to oxygen in its ground state and toluene; this is a spin forbidden reaction which has been reported only to compare the energy of the singlet isomers with that of the triplet ones. We can notice that the three isomers are almost degenerate with a slight preference for the first isomer. It is worth noting also that the DFT and CCSD(T) energies are in very good agreement suggesting that for the study of larger systems it could be possible to use DFT calculations. The loss of CH_3 or H from the very stable minimum 1OMIN1 are endothermic processes, as expected, as we can see from the values reported in Table 2.

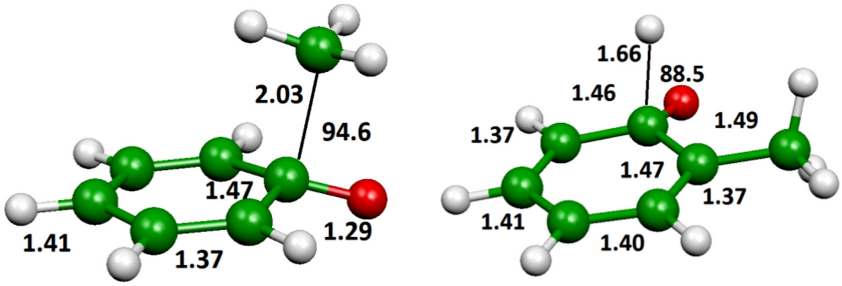

Fig. 5. Optimized geometries at ωB97XD/6-311+G(d,p) level of the saddle points for the loss of CH_3 from the ipso isomer (3OMIN5) and H from the *ortho* isomer (3OMIN6) in the $O(^3P)$+toluene PES. Bond lengths in Å, angles in degrees. Carbon in green, oxygen in red, hydrogen in white. (Color figure online)

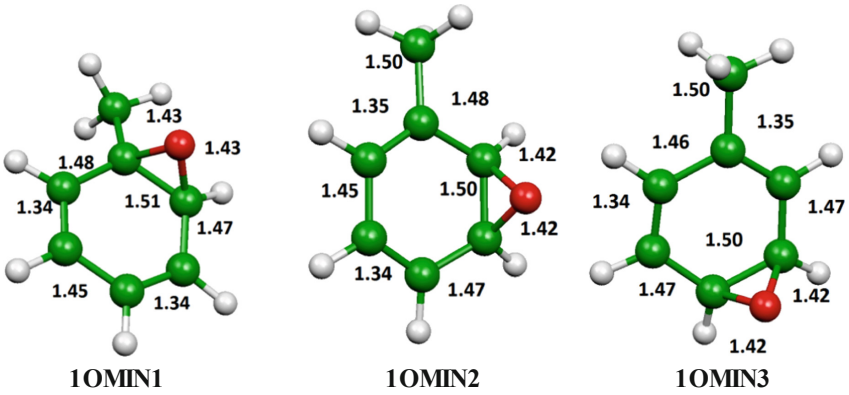

Fig. 6. Optimized geometries at ωB97XD/6-311+G(d,p) level of the minima for the attack of $O(^1D)$ to toluene. Bond lengths in Å. Carbon in green, oxygen in red, hydrogen in white. (Color figure online)

Table 1. Enthalpy changes and barrier heights (kcal/mol, 0 K) computed at the ωB97X-D/6-311+G(d,p), B3LYP/6-311+G(d,p), CCSD(T)/aug-cc-pVTZ//ωB97X-D/6-311+G(d,p) and CCSD(T)/aug-cc-pVTZ//B3LYP/6-311+G(d,p) levels of theory for selected reactions of $N(^2D)$ + toluene system.

	$\Delta H^0{}_0$	
	ωB97X-D (CCSD(T))	B3LYP (CCSD(T))
$N(^2D)+C_6H_5CH_3 \rightarrow$ 2NMIN1	−80.5 (−75.6)	−78.8 (−75.9)
$N(^2D)+C_6H_5CH_3 \rightarrow$ 2NMIN2	−80.1 (−74.9)	−78.6 (−75.2)
$N(^2D)+C_6H_5CH_3 \rightarrow$ 2NMIN3	−79.6 (−74.9)	−78.6 (−75.2)
	$\Delta H^0{}_0$	Barrier height
B3LYP		
$N(^2D)+C_6H_5CH_3 \rightarrow$ 2NMIN0	−30.2	
2NMIN0 → 2NMIN1	−48.6	2.6
ωB97X-D (CCSD(T))		
2NMIN1 – CH_3 → products	47.4 (43.4)	47.9 (45.3)
2NMIN1 – H → products	55.1 (51.8)	58.0 (53.3)
B3LYP		
2NMIN1 – CH_3 → products	40.4	43.6
2NMIN1 – H → products	53.7	54.6

Table 2. Enthalpy changes and barrier heights (kcal/mol, 0 K) computed at the ωB97X-D/6-311+G(d,p) and CCSD(T)/aug-cc-pVTZ//ωB97X-D/6-311+G(d,p) levels of theory for selected reactions of $O(^3P, ^1D)$ + toluene system. In parentheses CCSD(T) results.

	$\Delta H^0{}_0$	Barrier height
$O(^3P)+C_6H_5CH_3 \rightarrow$ 3OMIN1	−2.7 (−1.6)	
$O(^3P)+C_6H_5CH_3 \rightarrow$ 3OMIN2	−2.5 (−1.4)	
$O(^3P)+C_6H_5CH_3 \rightarrow$ 3OMIN3	−2.3 (−1.2)	
$O(^3P)+C_6H_5CH_3 \rightarrow$ 3OMIN4	−2.3 (−1.2)	
3OMIN1 → 3OMIN5	−14.5 (−11.2)	2.7 (6.8)
3OMIN2 → 3OMIN6	−15.7 (−11.5)	2.7 (6.1)
3OMIN3 → 3OMIN7	−14.5 (−10.4)	3.6 (7.0)
3OMIN4 → 3OMIN8	−14.8 (−10.3)	6.7 (9.9)
3OMIN5 – CH_3 → products	−7.2 (−7.0)	7.7 (8.1)
3OMIN6 – H → products	0.5 (0.5)	13.2 (11.5)
3OMIN7 – H → products	0.1 (0.1)	13.5 (11.8)
3OMIN8 – H → products	0.6 (0.7)	13.7 (12.1)
$O(^3P)+C_6H_5CH_3 \rightarrow$1OMIN1	−55.1 (−55.4)	
$O(^3P)+C_6H_5CH_3 \rightarrow$1OMIN2	−53.7 (−53.6)	
$O(^3P)+C_6H_5CH_3 \rightarrow$1OMIN3	−53.3 (−53.5)	
1OMIN1 – CH_3 →products	94.7 (95.1)	
1OMIN1 – H →products	100.6 (99.8)	

4 Conclusions

The study at *ab initio* level of the interaction of $N(^2D)$, $O(^3P)$ and $O(^1D)$ with toluene, performed using different methods in order to find a reasonable compromise between chemical accuracy and computational costs suggests that, while for geometry optimizations DFT methods are adequate, for energies, calculations of higher level are necessary in order to obtain accurate quantitative results, although even DFT methods can provide reasonable semi-quantitative results.

Acknowledgments. We acknowledge the MUR (Ministero dell'Università e della Ricerca) for "PRIN 2017" funds, project "Modeling and Analysis of carbon nanoparticles for innovative applications Generated dIrectly and Collected DUring combuSTion (MAGIC DUST)", Grant Number 2017PJ5XXX. SF and MR acknowledge the project "Indagini teoriche e sperimentali sulla reattività di sistemi di interesse astrochimico" funded with Fondo Ricerca di Base of the University of Perugia. MR thanks the Department of Civil and Environmental Engineering of the University of Perugia for allocated computing time within the project "Dipartimenti di Eccellenza 2018–2022".

References

1. Brezinsky, K.: The high-temperature oxidation of aromatic hydrocarbons. Prog. Energy Combust. **12**, 1–24 (1986)
2. Atkinson, R., Pitts, J.N.: Rate constants for the reaction of O(^{3}P) atoms with benzene and toluene over the temperature range 299–440 K. Chem. Phys. Lett. **63**, 485–489 (1979)
3. Nicovich, J.M., Gump, C.A., Ravishankara, A.R.: Rates of reactions of O(^{3}P) with benzene and toluene. J. Phys. Chem. **86**, 1684–1690 (1982)
4. Tappe, M., Schliephake, V., Wagner, H.G.: Reactions of benzene, toluene and ethylbenzene with atomic oxygen O(^{3}P) in the gas phase. Z. Phys. Chem. **162**, 129–145 (1989)
5. Cavallotti, C., et al.: Relevance of the channel leading to formaldehyde + triplet ethylidene in the O(^{3}P)+propene reaction under combustion conditions. J. Phys. Chem. Lett. **5**, 4213–4218 (2014)
6. Leonori, F., et al.: Experimental and theoretical studies on the dynamics of the O(^{3}P)+propene reaction: primary products, branching ratios, and role of intersystem crossing. J. Phys. Chem. C **119**, 14632–14652 (2015)
7. Gimondi, I., Cavallotti, C., Vanuzzo, G., Balucani, N., Casavecchia, P.: Reaction dynamics of O(^{3}P)+propyne: II. Primary products, branching ratios, and role of intersystem crossing from ab initio coupled triplet/singlet potential energy surfaces and statistical calculations. J. Phys. Chem. A **120**, 4619–4633 (2016)
8. Caracciolo, A., et al.: Combined experimental and theoretical studies of the O(^{3}P)+1-butene reaction dynamics: primary products, branching ratios and role of intersystem crossing. J. Phys. Chem. A **123**, 9934–9956 (2019)
9. Hörst, S. M.: Titan's atmosphere and climate. J. Geophys. Res. Planets **122**, 432–482 (2017)
10. Vuitton, V., Yelle, R.V., Anicich, V.G.: The nitrogen chemistry of Titan's upper atmosphere revealed. Astrophys. J. **647**, L175–L178 (2006)
11. Vuitton, V., Dutuit, O., Smith, M.A., Balucani, N.: Chemistry of Titan's atmosphere. In: Mueller-Wodarg, I., Griffith, C., Lellouch, E., Cravens, T. (eds.) Titan: Surface, Atmosphere and Magnetosphere, Cambridge University Press (2013)
12. Balucani, N.: Elementary reactions of N atoms with hydrocarbons: first steps towards the formation of prebiotic N-containing molecules in planetary atmospheres. Chem. Soc. Rev. **41**, 5473–5483 (2012)
13. Brown, R., Lebreton, J.P., Waite, J. (eds.): Titan from Cassini-Huygens. Springer, Nethelands (2010). https://doi.org/10.1007/978-1-4020-9215-2
14. Vuitton, V., Yelle, R.V., Cui, J.: Formation and distribution of benzene on Titan. J. Geophys. Res. **113**, E05007 (2008)
15. Loison, J.C., Dobrijevic, M., Hickson, K.M.: The photochemical production of aromatics in the atmosphere of Titan. Icarus **329**, 55–71 (2019)
16. Lavvas, P., et al.: Energy deposition and primary chemical products in Titan's upper atmosphere. Icarus **213**, 233–251 (2011)
17. Balucani, N., et al.: Combined crossed molecular beam and theoretical studies of the N(^{2}D) + CH_4 reaction and implications for atmospheric models of Titan. J. Phys. Chem. A **113**, 11138–11152 (2009)
18. Balucani, N., et al.: Cyanomethylene formation from the reaction of excited nitrogen atoms with acetylene: a crossed beam and ab initio study. J. Am. Chem. Soc. **122**, 4443–4450 (2000)
19. Balucani, N., Cartechini, L., Alagia, M., Casavecchia, P., Volpi, G.G.: Observation of nitrogen-bearing organic molecules from reactions of nitrogen atoms with hydrocarbons: a crossed beam study of N(^{2}D) + ethylene. J. Phys. Chem. A **104**, 5655–5659 (2000)
20. Balucani, N., et al.: Formation of nitriles and imines in the atmosphere of Titan: combined crossed-beam and theoretical studies on the reaction dynamics of excited nitrogen atoms N(^{2}D) with ethane. Faraday Discuss. **147**, 189–216 (2010)

21. Balucani, N., et al.: Combined crossed beam and theoretical studies of the $N(^2D) + C_2H_4$ reaction and implications for atmospheric models of Titan. J. Phys. Chem. A **116**, 10467–10479 (2012)
22. Rosi, M., Falcinelli, S., Balucani, N., Casavecchia, P., Skouteris, D.: A theoretical study of formation routes and dimerization of methanimine and implications for the aerosols formation in the upper atmosphere of Titan. Lect. Notes Comp. Sci. **7971**, 47–56 (2013)
23. Balucani, N., Pacifici, L., Skouteris, D., Caracciolo, A., Casavecchia, P., Rosi, M.: A theoretical investigation of the reaction $N(^2D) + C_6H_6$ and implications for the upper atmosphere of Titan. Lect. Notes Comp. Sci. **10961**, 763–772 (2018)
24. Rosi, M., et al.: A computational study on the insertion of $N(^2D)$ into a C—H or C—C bond: the reactions of $N(^2D)$ with benzene and toluene and their implications on the chemistry of Titan. Lect. Notes Comp. Sci. **12251**, 744–755 (2020)
25. Balucani, N., et al.: A computational study of the reaction $N(^2D) + C_6H_6$ leading to pyridine and phenylnitrene. LNCS **11621**, 316–324 (2019)
26. Chai, J.-D., Head-Gordon, M.: Long-range corrected hybrid density functionals with damped atom-atom dispersion corrections. Phys. Chem. Chem. Phys. **10**, 6615–6620 (2008)
27. Chai, J.-D., Head-Gordon, M.: Systematic optimization of long-range corrected hybrid density functionals. J. Chem. Phys. **128**, 084106 (2008)
28. Becke, A.D.: Density functional thermochemistry. III. The role of exact exchange. J. Chem. Phys. **98**, 5648–5652 (1993)
29. Stephens, P.J., Devlin, F.J., Chablowski, C.F., Frisch, M.J.: Ab initio calculation of vibrational absorption and circular dichroism spectra using density functional force fields. J. Phys. Chem. **98**, 11623–11627 (1994)
30. Krishnan, R., Binkley, J.S., Seeger, R., Pople, J.A.: Self-consistent molecular orbital methods. XX. A basis set for correlated wave functions. J. Chem. Phys. **72**, 650–654 (1980)
31. Frisch, M.J., Pople, J.A., Binkley, J.S.: Self-consistent molecular orbital methods 28. Supplementary functions for Gaussian basis sets. J. Chem. Phys. **80**, 3265–3269 (1984)
32. Gonzalez, C., Schlegel, H.B.: An improved algorithm for reaction path following. J. Chem. Phys. **90**, 2154–2161 (1989)
33. Gonzalez, C., Schlegel, H.B.: Reaction path following in mass-weighted internal coordinates. J. Phys. Chem. **94**, 5523–5527 (1990)
34. Bartlett, R.J.: Many-body perturbation theory and coupled cluster theory for electron correlation in molecules. Ann. Rev. Phys. Chem. **32**, 359–401 (1981)
35. Raghavachari, K., Trucks, G.W., Pople, J.A., Head-Gordon, M.: Quadratic configuration interaction. A general technique for determining electron correlation energies. Chem. Phys. Lett. **157**, 479–483 (1989)
36. Olsen, J., Jorgensen, P., Koch, H., Balkova, A., Bartlett, R.J.: Full configuration–interaction and state of the art correlation calculations on water in a valence double-zeta basis with polarization functions. J. Chem. Phys. **104**, 8007–8015 (1996)
37. Dunning, T.H., Jr.: Gaussian basis sets for use in correlated molecular calculations. I. The atoms boron through neon and hydrogen. J. Chem. Phys. **90**, 1007–1023 (1989)
38. de Petris, G., Cacace, F., Cipollini, R., Cartoni, A., Rosi, M., Troiani, A.: Experimental detection of theoretically predicted N_2CO. Angew. Chem. **117**, 466–469 (2005)
39. De Petris, G., Rosi, M., Troiani, A.: SSOH and HSSO radicals: an experimental and theoretical study of $[S_2OH]^{0/+/-}$ species. J. Phys. Chem. A **111**, 6526–6533 (2007)
40. Bartolomei, M., et al.: The intermolecular potential in NO–N_2 and $(NO–N_2)^+$ systems: implications for the neutralization of ionic molecular aggregates. PCCP **10**, 5993–6001 (2008)
41. Leonori, F., et al.: Observation of organosulfur products (thiovinoxy, thioketene and thioformyl) in crossed-beam experiments and low temperature rate coefficients for the reaction $S(^1D) + C_2H_4$. PCCP **11**, 4701–4706 (2009)

42. Leonori, F., et al.: Crossed-beam and theoretical studies of the $S(^1D) + C_2H_2$ reaction. J. Phys. Chem. A **113**, 4330–4339 (2009)
43. De Petris, G., Cartoni, A., Rosi, M., Barone, V., Puzzarini, C., Troiani, A.: The proton affinity and gas-phase basicity of sulfur dioxide. ChemPhysChem **12**, 112–115 (2011)
44. Berteloite, C., et al.: Low temperature kinetics, crossed beam dynamics and theoretical studies of the reaction $S(^1D) + CH_4$ and low temperature kinetics of $S(^1D) + C_2H_2$. Phys. Chem. Chem. Phys. **13**, 8485–8501 (2011)
45. Rosi, M., Falcinelli, S., Balucani, N., Casavecchia, P., Leonori, F., Skouteris, D.: Theoretical study of reactions relevant for atmospheric models of Titan: interaction of excited nitrogen atoms with small hydrocarbons. LNCS **7333**, 331–344 (2012)
46. Skouteris, D., Balucani, N., Faginas-Lago, N., Falcinelli, S., Rosi, M.: Dimerization of methanimine and its charged species in the atmosphere of Titan and interstellar/cometary ice analogs. Astron. Astrophys. **584**, A76 (2015)
47. Falcinelli, S., Rosi, M., Cavalli, S., Pirani, F., Vecchiocattivi, F.: Stereoselectivity in autoionization reactions of hydrogenated molecules by metastable gas atoms: the role of electronic couplings. Chem. Eur. J. **22**, 12518–12526 (2016)
48. Troiani, A., Rosi, M., Garzoli, S., Salvitti, C., de Petris, G.: Vanadium hydroxide cluster ions in the gas phase: bond-forming reactions of doubly-charged negative ions by SO_2-promoted V-O activation. Chem. Eur. J. **23**, 11752–11756 (2017)
49. Rosi, M., et al.: An experimental and theoretical investigation of 1-butanol pyrolysis. Front. Chem. **7**, 326 (2019). https://doi.org/10.3389/fchem.2019.00326
50. Moore, C. E.: Atomic Energy Levels, Natl. Bur. Stand. (U.S.) Circ. N. 467. U.S., GPO, Washington (1949)
51. Frisch, M. J., et al.: Gaussian 09, Revision A.02, Gaussian, Inc., Wallingford (2009)
52. Flükiger, P., Lüthi, H. P., Portmann, S., Weber, J., MOLEKEL 4.3, Swiss Center for Scientific Computing, Manno (Switzerland), 2000–2002
53. Portmann, S., Lüthi, H.P.: MOLEKEL: an interactive molecular graphics tool. Chimia **54**, 766–769 (2000)
54. Chin, C.-H., Zhu, T., Zhang, J.Z.H.: Cyclopentadienyl radical formation from the reaction of excited nitrogen atoms with benzene: a theoretical study. PCCP (2021), online version. https://doi.org/10.1039/d1cp00133g